A&A 402, 253–265 (2003)
DOI: 10.1051/0004-6361:20030224
© ESO 2003

Astronomy & Astrophysics

Stellar and circumstellar activity of the Be star ω CMa*

I. Line and continuum emission in 1996–2002

S. Štefl[1], D. Baade[2], Th. Rivinius[2,3], S. Otero[4,5], O. Stahl[3], A. Budovičová[1], A. Kaufer[6], and M. Maintz[3]

[1] Astronomical Institute, Academy of Sciences, 251 65 Ondřejov, Czech Republic
[2] European Southern Observatory, Karl-Schwarzschild-Str. 2, 85748 Garching bei München, Germany
[3] Landessternwarte Königstuhl, 69117 Heidelberg, Germany
[4] Liga Iberoamericana de Astronomia, Buenos Aires, Argentina
[5] Centro de Estudios Astronomicos, Mar Del Plata, Argentina
[6] European Southern Observatory, Casilla 19001, Santiago 19, Chile

Received 17 October 2002 / Accepted 31 January 2003

Abstract. Echelle spectroscopy and mostly unaided-eye photometry of the southern Be star ω CMa were obtained in the period 1996–2003. The monitoring is bracketed by two brightenings by $0\overset{m}{.}4$–$0\overset{m}{.}5$. The results of a literature search suggest that such phases occur about once a decade and have various commonalities. Along with these photometric events goes enhanced line emission. This is due to an increased total mass of the disk as well as to a change in its density profile. The models by Poeckert & Marlborough (1978, 1979) imply that the enhanced continuum flux originates from the inner disk. Higher-order Balmer line emission is correlated with brightness. The increase in Hα is retarded by some months, possibly indicating a time delay in filling up and ionizing the outer disk. In the $(U-B)$ vs. $(B-V)$ colour diagram and the D_{54} vs. D_{34} Balmer decrement diagram the path from the ground to the bright state is distinct from the return path. This could result from the bulk of the disk matter being in the outer (inner) disk during the photometric ground (high) state, while the two transitions between the two states are both due to changes progressing radially outward. Some μ Cen-like outbursts (Rivinius et al. 1998c) seem to occur in all phases. It is conceivable that the build-up of the inner disk is caused by more frequent or more effective outbursts. During the photometric bright state various other phenomena gain in prominence and suggest this to be a phase of increased activity. Of particular interest, but possibly only apparently related to this phase, are absorption components at redshifts well beyond the range covered by the combination of rotation and nonradial pulsation.

Key words. stars: activity – stars: circumstellar matter – stars: emission-line, Be – stars: individual: ω 28 CMa

1. Introduction

Classical Be stars owe the emission lines defining this class of stars to a (mainly rotationally supported – Rivinius et al. 1999) circumstellar disk. Often, the disks undergo slow cyclic variations of the violet-to-red emission peak ratio, V/R, which find a convincing explanation in global one-armed oscillations (Okazaki 1997). Especially among the early spectral subclasses, long-term variations (over years to decades) of the equivalent widths (EW) of the emission lines are common, with optical emission lines sometimes even becoming temporarily undetectable.

In recent years, mounting observational evidence has been presented suggesting that the life cycle of the disks of (early-type) Be stars is influenced strongly by outburst events of the central star. With only limited observational data being available and quantitative estimates not having been made, the most extreme hypothesis is not excluded that the build-up of a disk is entirely due to discrete star-to-disk mass transfer events. Since Be stars typically do not rotate at more than 80% of the critical velocity, the required accompanying angular momentum transfer is the key challenge for any model. Whatever the disk forming processes are, they are counter-acted by one or several other processes, which demolish the disk, mainly progressing from its inner boundary (Rivinius et al. 2001).

Which observational phenomena may or may not be called an outburst is far from clear. Rivinius et al. (1998a) established that the outbursts of μ Cen exhibit a fairly homogeneous temporal profile and later Rivinius et al. (2001) found that very similar events take place in quite a few other early-type Be stars. The famous spectacular increase in visual magnitude and Balmer emission strength observed in γ Cas in 1936–1939 (Cleminshaw 1936; Huffer 1939) has also been called an

Send offprint requests to: S. Štefl,
e-mail: sstefl@pleione.asu.cas.cz

* Based on observations collected at the European Southern Observatory at La Silla, Chile, ESO (proposal nos. 55.D–0502, 56.D–0381, 58.D–0697, 62.H-0319, 64.H-0548).

Article published by EDP Sciences and available at http://www.aanda.org or http://dx.doi.org/10.1051/0004-6361:20030224

outburst. But it is not known whether this episode was a μ Cen analog with scaled-up duration and amplitude, whether it was the result of a dense series of normal-sized μ Cen-like outbursts, or whether it was a completely different kind of event.

In shell stars, which are Be stars viewed equator-on and through the disk, outbursts could, in addition to enhanced line emission, reveal themselves by increased absorption. Steady-state model calculations by Poeckert & Marlborough (1978) lead to the expectation that pole-on stars brighten during an outburst whereas shell stars fade. The largest suitable photometric database analyzed to date, namely the one from Hipparcos, shows recurrent short as well as long-lived brightenings and fadings (Hubert & Floquet 1998).

Some outbursts repeat cyclically. Rivinius et al. (1998a,b) found the times of positive resonances between two of the strongest non-radial pulsation (*nrp*) modes to correlate with the times of emission outbursts of the southern Be star μ Cen. Harmanec (1984) speculated that shell phases in the Be star o And are triggered by a companion in the binary system and predicted the emission outbursts to repeat cyclically every 8.5 years. Observations in subsequent years, however, did not confirm his expectation, and only 28 Cyg (Tubbesing et al. 2000) has so far shown indications of a behaviour similar to the one of μ Cen. Accordingly, whether or not outbursts repeat regularly should probably not play a major role for their understanding.

The bright southern Be star ω CMa (28 CMa, $v \sin i = 80\,\mathrm{km\,s^{-1}}$, Slettebak 1982) is one of the first early-type stars for which rapid spectroscopic variations on a time scale of one day were detected both in radial velocities (Abt & Biggs 1972) and line profiles (Baade 1982, 1984b). Later observations showed that in addition to the very stable 1.37-d period (e.g. Harmanec 1998) a transient 1.47-d period can be isolated especially in lines (partly) formed in the inner disk (Štefl et al. 1998, 2000b).

Hipparcos recorded three brightenings 330 and 200 days apart (Hubert & Floquet 1998) of which the last one actually marks the ascent to another major brightening. The emission activity over more than 40 years until 1995 was described by Harmanec (1998), who also compiled and analyzed the published radial velocities. Further detailed information on the star, including the photometric variability, can be found in Štefl et al. (1999).

This series of papers presents a multi-line analysis of more than 400 new echelle spectra, obtained mainly with the Heros and Feros spectrographs, in a synopsis with a long-term, mostly visual, photometric monitoring of the star. The aims of this first paper are:

- to describe the emission activity of the star in the period 1996–2002,
- to search for any spectroscopic signatures accompanying two strong brightenings observed in 1996 and 2001/2002,
- to establish whether and, if yes, which commonalities exist between these long-term variations and μ Cen-like outbursts.

The database is described in Sect. 2, from which Sect. 3 distills the characteristics of both photometric and spectroscopic long-term variations. Section 4 focuses on additional phenomena occurring mainly during the photometric maxima in 1996 and 2001/2002. The discussion and some qualitative interpretation are offered in Sect. 5, while Sect. 6 attempts to assemble the results to a chronology of a typical long-term disk cycle.

Paper II (Štefl et al., in preparation) of this series will be devoted to the analysis of the short-periodic line profile variability (*lpv*) and their distinction from transient periods. Paper III (Maintz et al., in preparation) will use these results to model the *lpv* as non-radial pulsation (*nrp*); it will also derive the fundamental stellar parameters and put them in a perspective with the results of other methods. All observational data will be published in Paper IV (Štefl et al., in preparation).

2. Observations and their reduction

2.1. New spectroscopy

This study is based on five spectroscopic observing runs (D, E, G, I, L in Table 1) at ESO's La Silla Observatory between 1996 and 2002 and a number of additional single spectra taken at various occasions. The ESO 0.5-m Telescope and the Heros spectrograph were used in two of the main runs, the ESO 1.5 m Telescope and the Feros spectrograph for the remaining 1999–2002 observations. Table 1 summarizes the main characteristics of the data sets used.

Heros (**H**eidelberg **E**xtended **R**ange **O**ptical **S**pectrograph) was described by Kaufer (1998). The spectral resolving power, $\lambda/\Delta\lambda$, is 20 000 in both channels, which together cover the spectral range 3450–8620 Å. More details on the spectrograph can be found, e.g., in Rivinius et al. (1998c).

The signal-to-noise ratio (S/N) per pixel was derived as the inverse of the rms in units of the continuum in the wavelength range 4760–4800 Å. In the case of Heros it was of the order of 130 early in 1996 but typically 150 after a more sensitive CCD was installed in the blue channel in May, 1996. A reduction of the exposure times by about one third was achieved after a more efficient fiber link and microlens were put into place in 1997.

A customized MIDAS echelle package described in detail by Stahl et al. (1995) was used for the Heros data reduction. An enhanced adaptation of the MIDAS TSA package developed by AK was used for the one- and two-dimensional time series analysis of the spectral variability.

The 1999–2002 observations were made with the ESO 1.5 m Telescope and the Feros spectrograph. The description of the spectrograph can be found in Kaufer et al. (1997, 1999). The data were reduced by means of the Feros pipeline software (Stahl et al. 1999).

2.2. New photometry

A modified version of the historical Argelander method (Hirshfeld & Sinnott 1985) was applied in visual observations carried out by SO at Buenos Aires, Argentina in the period 1997 April–2003 January. Visual magnitudes are determined using a grid of standard stars defining the magnitude scale (see Table 2) and cone vision, which increases the ability to

Table 1. Spectroscopic data sets.

Data set	Observing season	JD 2 400 000+	Telescope	No spect./ no. nights	Instrument	Typical S/N	Resolving power	Spectral range [Å]	Ref.
A	1982 Oct./	45244-357	ESO CAT	20/10	CES	350	100 000	4457–4492	1
	1983 Jan.			5/4	CES	400	100 000	4841–4879	1
B	1994 Nov.	49667-672	ESO CAT	11/3	CES	300	60 000	6649–6707	2
C	1996 Jan.	50093-101	ESO CAT	264/8	CES	300	65 000	6641–6715	2
D	1996 Jan.-Apr.	50102-205	ESO 0.5 m	91/102	Heros	120	20 000	3450–8620	o
E	1997 Jan.-Apr.	50449-554	ESO 0.5 m	119/104	Heros	155	20 000	3450–8620	o
F	1998 Mar.	50877	MSO 74″	1/1	echelle	<100	53 333	4340–6700	o
G	1999 Jan.	51183-201	ESO 1.5 m	32/17	Feros	200	48 000	3600–9200	o
H	1999 Jun.	51302	ESO 0.5 m	1/1	Heros	145	20 000	3450–8620	o
I	2000 Jan.	51554–570	ESO 1.5 m	65/17	Feros	330	48 000	3600–9200	o
J	2000 Feb.	51596	Mt John 1. m	1/1	echelle	130	48 000	4084–7120	o
K	2001 Oct.	52205-206	ESO 1.5 m	2/3	Feros	200	48 000	3600–9200	o
L	2002 Jan.	52277-277	ESO 1.5 m	128/2	Feros	210	48 000	3600–9200	o
M	2002 Feb.-Mar.	52316-339	ESO 1.5 m	3/2	Feros	210	48 000	3600–9200	o

References: 1 – Baade (1984b), 2 – Štefl et al. (2000a), o – not previously published data.

Table 2. ω CMa and the sequence of comparison stars used for visual photometry.

Star	HR	HD	α(2000)	δ(2000)	V	$B-V$
ω CMa	2749	56139	$07^h\ 15^m$	$-26°\ 46'$	3.54–4.18	−0.10–−0.20
(14) ζ Lep	1998	38678	$05^h\ 47^m$	$-14°\ 49'$	3.55	0.10
(16) η Lep	2085	40136	$05^h\ 56^m$	$-14°\ 10'$	3.72	0.33
k Pup	2948/9	61555/6	$07^h\ 39^m$	$-26°\ 48'$	3.82	−0.16
11 Pup	3102	65228	$07^h\ 57^m$	$-22°\ 53'$	4.20	0.72
3 Pup	2996	62623	$07^h\ 44^m$	$-28°\ 57'$	3.96	0.18
c Pup	3017	63032	$07^h\ 45^m$	$-37°\ 58'$	3.60	1.73
a Pup	3080	64440	$07^h\ 52^m$	$-40°\ 35'$	3.71	1.03
χ Car	3117	65575	$07^h\ 57^m$	$-52°\ 59'$	3.46	−0.19

distinguish small magnitude differences for bright stars. With the help of several comparison stars distributed all around the variable, the effect of differential extinction and colour response can be roughly calibrated. This calibration technique implies that more standard stars are needed and their selection follows different criteria than for the photoelectric photometry. For naked eye observations, standard stars up to 30° from the variable are still suitable for brightness estimates. The sequence forms a sufficiently dense brightness scale (with a magnitude difference smaller than 0.2) that minimizes the deviations from the standard system.

The comparison stars used at any given epoch are selected according to their respective zenith distance. Higher weight is given to comparison stars with a colour index close to that of the variable. Although they are very far away from ω CMa by the rules of photoelectric photometry, η and ζ Lep meet these requirements well. Therefore, they are relied on as the primary comparison stars, except for the end of the observing season when their zenith distances exceed the fixed limit well before ω CMa. Then, more emphasis has to be given to the standard stars in Puppis which are located in more nearby fields but have less favourable colours. Errors due to differential extinction were further minimized by restricting the observations to zenith distance less than about 45°.

The nightly values were derived as averages from several observations. The error is about $0\overset{m}{.}1$ for the observations obtained in 1997–2000. During 2000 a more efficient method was adopted and the error was decreased to $\sim 0\overset{m}{.}05$ in good photometric nights and to about $0\overset{m}{.}08$ in nights of inferior observing conditions. The error is derived from the quality of the night, the scatter of individual values and the magnitude difference between the comparison stars. Simultaneous visual and photoelectric observations of δ Sco (Otero et al. 2001) have confirmed these error estimates as realistic. Photoelectric observations obtained in 2000 February and described below provide another check of the visual observations. The mean difference between the two data sets is $\sim 0\overset{m}{.}03$.

New photoelectric photometry was obtained with the 0.6-m Craftsman Telescope of the Mount John Observatory, New Zealand, during 4 nights in the period

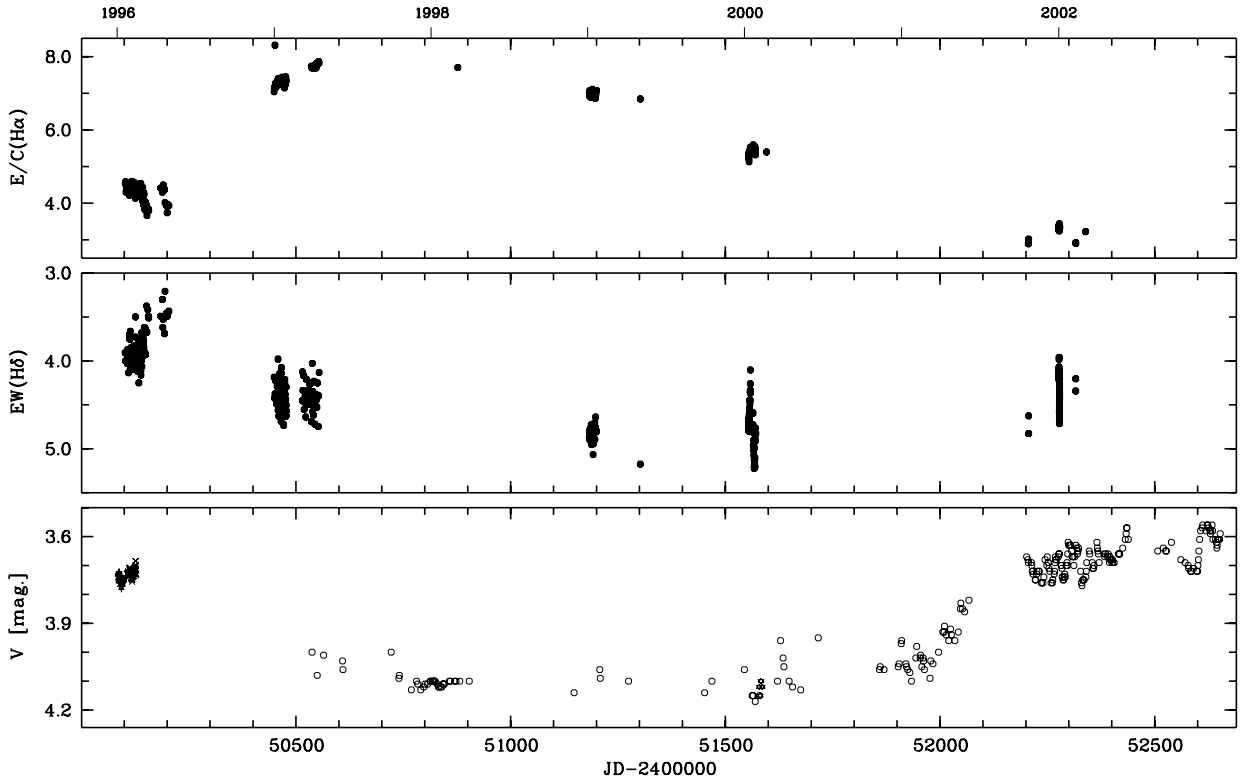

Fig. 1. Long-term variability of ω CMa in the period January, 1996–January, 2003. Bottom panel: V magnitudes derived from observations in four photometric systems: visual observations by SO (o) and photoelectric data in *uvby* obtained at the SAAO (+ Štefl et al. 2000a), Geneva system data obtained at La Silla (x Štefl et al. 2000a) and *uvby* magnitudes obtained at Mt. John Observatory (⋆). Systematic differences between the above data sets should not be larger than a few hundredth of a magnitude. Middle panel: Equivalent widths of Hδ (blended with He I 4120 in the red wing). For constant photospheric contribution, lower equivalent widths correspond to increased emission in the wings (see also Fig. 3). Top panel: Peak height of the Hα emission relative to the ambient continuum flux, E/C.

Table 3. Standard magnitudes and colours of the comparison and check stars used for the Mt. John photoelectric photometry.

HR	HD	y	$b-y$	c_1	m_1
2497	49028	6.531	−0.054	0.493	0.121
2769	56733	5.817	−0.067	−0.026	0.112

February 2–11, 2000. The single-channel photometer was used with Strömgren *uvby* filters. HR 2497 and HR 2769 served as comparison and check star, respectively (cf. Table 3). The data were reduced with the help of the HEC 22 Fortran program (Harmanec & Horn 1998). Because of the very limited number of useful observing nights and unstable weather conditions, it was not possible to observe standard stars, and only differential magnitudes were derived.

2.3. Archival spectra

The 275 He I 6678 high resolution line profiles published by Štefl et al. (2000a) and the 25 obtained before by Baade (1984a) were included in the analysis. The latter were re-reduced and will also be published in Paper IV.

3. Long-term variability

The long-term variability of the V magnitude, the Hδ equivalent width and the Hα peak height, E/C (in units of the ambient continuum), in the period 1996–2002 is shown in Fig. 1. For a comprehensive overview of the emission activity of ω CMa before 1996 the work by Harmanec (1998) is referred to.

3.1. Major photometric brightening cycles

The period covered by this study is bracketed by two major brightenings in 1995/1996 and 2001/2002 during which the V magnitude increased by about $0\overset{m}{.}4$–$0\overset{m}{.}5$. Between these bright phases, the V magnitude stays near a "ground state" of about $4\overset{m}{.}1$ and displays occasional flares of about $0\overset{m}{.}1$. The first of these two bright phases seems to have been observed already by Štefl et al. (Fig. 1, 1999) in 1994 December through 1995 January and in 1995 November. On the basis of these data strings only, it would not be possible to firmly distinguish between their belonging to one and the same extended bright phase or presenting two separate shorter brightenings. However, a detailed compilation of all published photometric data (see Fig. 2 and Otero et al., in preparation) suggests that the observations by Štefl et al. were obtained when the bright phase was already well developed, and that it was the same bright phase that was observed by Hipparcos (Perryman et al. 1997) to have begun around 1992 April.

A similar major brightening by about $0\overset{m}{.}4$ was observed in broad-band UBV photometry on JD 2 445 500 ± 100 (see Sect. 3.4 and references therein). This gives separations

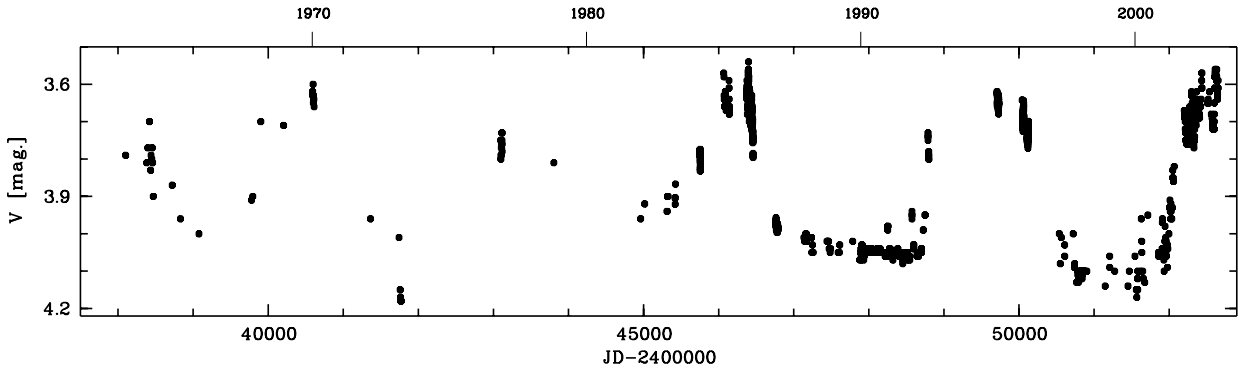

Fig. 2. Long-term brightness variations of ω CMa in the period 1964–2002 (from Otero et al., in preparation). The compilation includes visual observations by Otero (this paper) and photolectric observations obtained in the LTPV (Manfroid et al. 1991, 1995 and Sterken et al. 1993), Hipparcos project (Perryman et al. 1997) and those published by Feinstein (1975), van Hoof (1975), Baade (1979, 1982), Stagg (1987), Dachs et al. (1988), and Štefl et al. (2000a, and this paper).

between photometric high states of 8.8 and 9.0 years, respectively. The starting dates of the high states and consequently also their separations and durations can be only roughly estimated because of missing data and the slow rise of brightness. Before 1982, the available data are too scarce to determine temporal characteristics of additional discrete high phases (see Fig. 2), but they are not in contradiction with the assumption that phases of high brightness appear cyclicly on a time scale of 7–9 years. Figure 2 also suggests the mean brightness in the ground photometric state to be monotonically decreasing by about $0\overset{\mathrm{m}}{.}1$ in 15 years.

The small number of properly observed major brightenings permits only a limited generalized pattern to be derived: they have an amplitude of $0\overset{\mathrm{m}}{.}4$–$0\overset{\mathrm{m}}{.}5$, a rise time of 300–500 days, a subsequent plateau of 1.5–3.5 years and a rather steep decline. Associated with the photometric high state seem to be certain phenomena such as cyclic brightness and equivalent width variations on a time scale of 20 days (see Sect. 4.1) and transient periodicities in some spectral lines, see Štefl et al. (1998, 2000b) and Paper II. On this basis, one would guess the present bright phase to last through the end of 2003 or even into 2004.

The present as well as the Hipparcos photometry (Perryman et al. 1997) contain several examples of smaller brightenings with amplitudes of about $0\overset{\mathrm{m}}{.}1$. Insufficient spectroscopic coverage and the lower accuracy of the visual photometry before JD 2 451 900 do not permit a search for some regularity in the occurrence of small brightenings, which seem to last for 10–30 days. Compared with μ Cen, outbursts/brightenings appear to be less frequent in ω CMa (see also Hubert & Floquet 1998, Table 3).

Being a pole-on star, ω CMa provides an example of the so-called positive correlation between light and emission strength variations as derived by Harmanec (1983) from other Be stars: the stronger the HI emission, the brighter the star. However, the better sampling of the data in Fig. 1 than the one available to Harmanec reveals that in 28 CMa this correlation exists for the equivalent width of Hδ whereas the maximum Hα peak height lags the photometric maximum by roughly 500 days. The long-term variability of Hδ takes place mostly in the wings

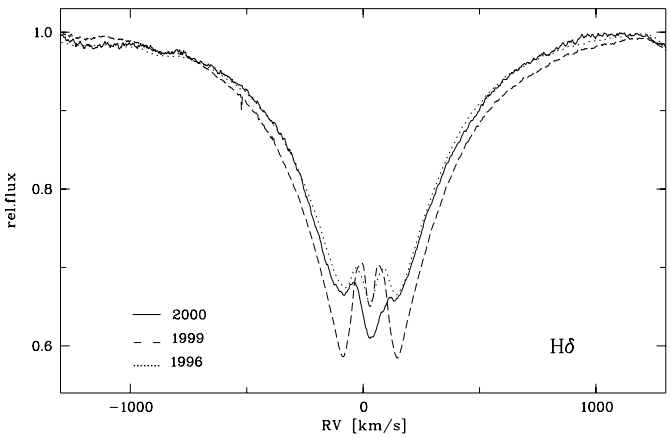

Fig. 3. Variations of the wings of Hδ between phases of high (1996, 2000) and base-line (1999) visual brightness. Mean seasonal profiles are plotted. The difference between the 1996 and 2000 profiles is also indicative of the uncertainty of the placement of the continuum

of the emission as well as of the absorption component (Fig. 3). Because the spectra are not flux calibrated, they had to be normalized to the continuum. As a result, it is likely that some fraction of the line profile variability reflects only continuum variations.

The Hδ EW also shows more rapid fluctuations. They can only partly be attributed to rectification errors, which can be as high as 10–15% for Heros and <5% for Feros data. The most prominent secondary variability occurs within days, causing the vertical spread in Fig. 1. Inspection of the corresponding profiles discloses a short-term variability of the violet-to-red emission strength ratio, V/R, the equivalent width being smallest when both peaks are about equally strong. Such V/R variability is associated both with the 1.37-d period of the permanently present nonradial pulsation as well as with the transient period(s) around 1.47d. In addition, the Hδ EW seems to share most of the variations described in more detail in Sect. 4.1 for the Hα EW.

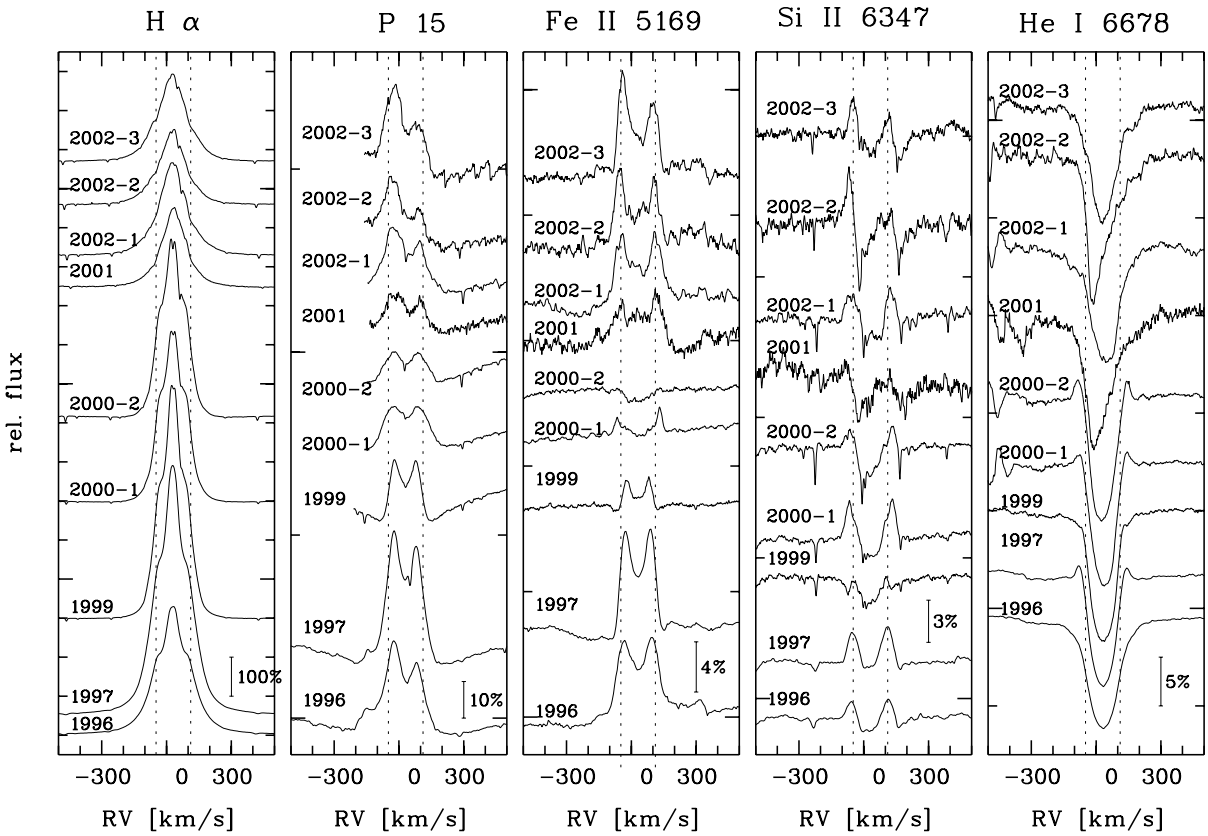

Fig. 4. From left to right, representative averaged profiles of lines formed in, or having a contribution from, the circumstellar disk. The lines are roughly sorted by distance of formation from the star. The dotted lines indicate $\pm v \sin i = 80\,\mathrm{km\,s^{-1}}$, corrected for the systemic velocity of the star of $31\,\mathrm{km\,s^{-1}}$ derived by Štefl et al. (1999). Asymmetric profiles represent the observing runs with spectra inhomogeneously distributed in phase. A weak peak in the blue wing of P15 results from a blend with the Ca II 8542.09. Similarly both wings of Fe II 5169 are influenced by blends with weaker Fe II lines. Note that the flux scales are different for different spectral lines.

3.2. Spectroscopic variations

Having been obtained in a small number of observing runs, the available spectroscopic data are not suitable to extract any slow continuous variation other than the long cycle shown in Figs. 1 and 2. Only season-to-season differences and variations within each observing run (ranging from 2 days to 3 months in length) can be searched for. Figure 4 shows the variation of seasonal averages of selected emission line profiles. The variability of derived parameters within each season is illustrated in Fig. 5 by the examples of the Hα E/C ratio, the equivalent widths of O I 8446 and Fe II 5169, and the separation of the violet and red emission peaks of Fe II 5169. Rivinius et al. (1998c) found these parameters to be the most suitable ones to identify and describe line emission outbursts in μ Cen. But only two details in Fig. 5 are reminiscent of the μ Cen scheme:

– During the high-brightness phase in 1996, the strength of most emission lines dropped twice, namely around JD 2 450 140 and JD 2450172, by various amounts (20% in Hα peak height) and after about 25 days recovered their previous level. These could be precursor phases of μ Cen-like outbursts.
– The very large separation of the emission peaks of metallic lines during the first part of the 2000 run suggests that the observations were taken shortly after an outburst. The brightness was at its ground state, with some occasional spikes, which might be outbursts. Although the ejection velocity was high, the relative increase in the disk mass was apparently small. The Hα peak height increased only very little and within days returned to its previous value while the Fe II had even become almost invisible after only 6 days.

It should be noted that the description of μ Cen-like outbursts by Rivinius et al. (1998c) is based on observations when μ Cen had little persistent emission. Therefore, the much larger underlying main emission of ω CMa and the implied presence of a more fully developed disk make a direct comparison difficult.

3.3. Fe II V/R variations

When the brightness of ω CMa is at its ground state, e.g. in 1999, the characteristics of Fe II emission lines such as V/R ratio, peak separation or radial velocities only show small variations by ±1% on a time scale of weeks to months. In contrast, during a photometric high state, these parameters vary by up to 10% on a time scale of days. Figure 6 illustrates different emission profiles of Fe II 5317 obtained during the 1996 brightness maximum. The whole variety of profiles with stronger blue or red peak, as well as those with a third weak central peak, could

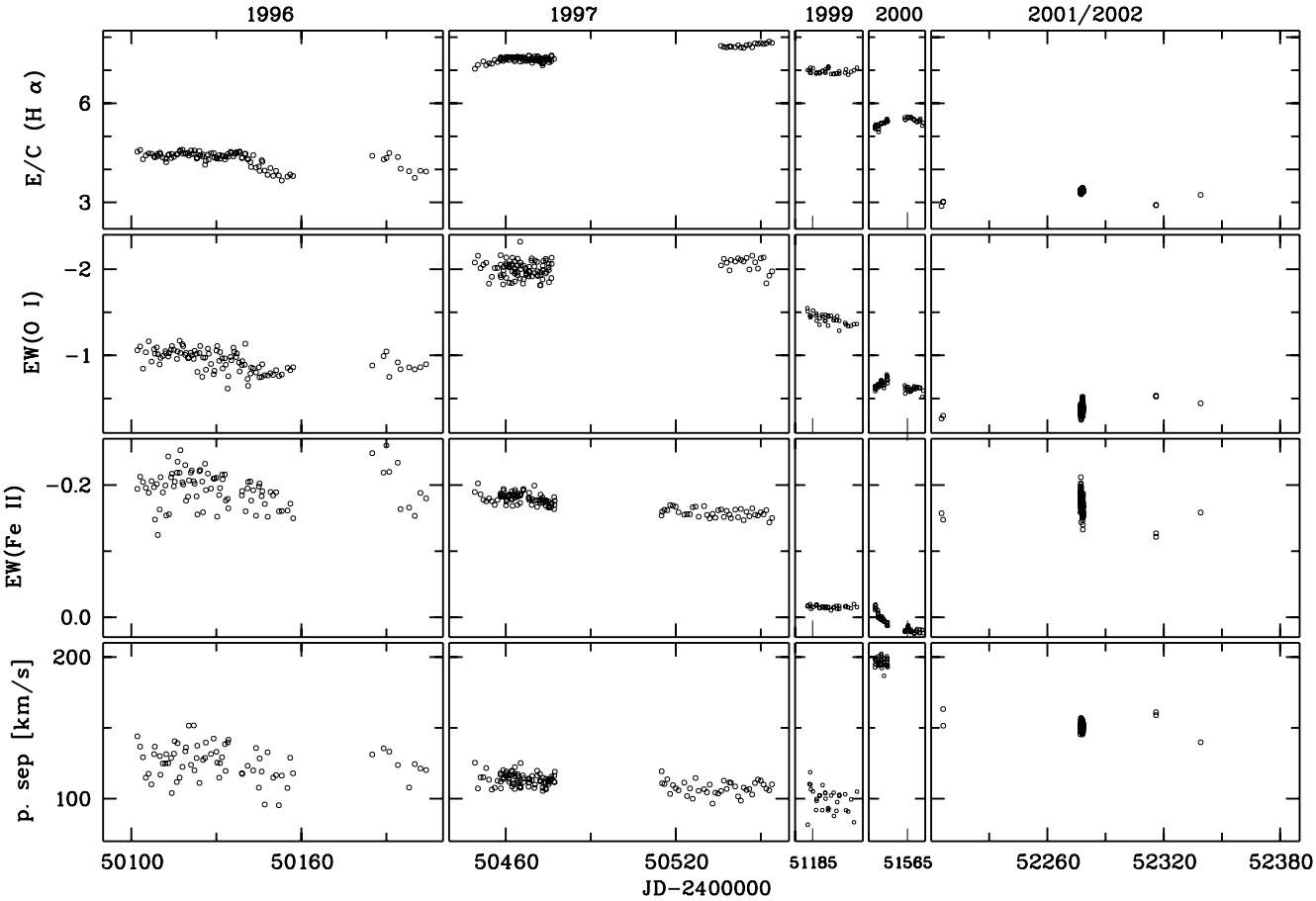

Fig. 5. Emission line characteristics during the main observing runs. From top to bottom: Hα E/C in units of the ambient continuum, equivalent width of O I 8446 Å (blended with P17), equivalent width of Fe II 5169 Å and separation of the emission peaks of Fe II 5169 Å.

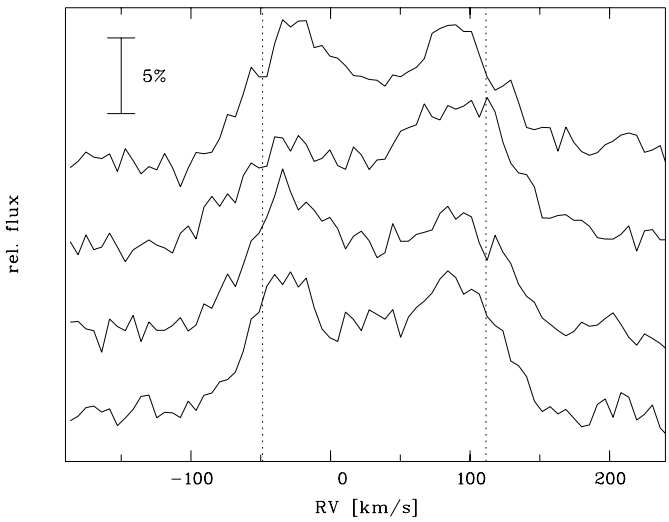

Fig. 6. Examples of the Fe II 5317 emission profile during the 1996 photometric maximum. Significant variations on a time scale of days are apparent. The profiles were obtained on JD 2 450 106.06, 2 450 108.25, 2 450 109.03 and 2 450 110.03, from top to bottom.

be observed over about 4 days. A detailed time series analysis of the emission line variations will be included in Paper II.

3.4. Colour variations

The visual photometry of this study does not permit the question of colour variations to be answered, which could provide important diagnostics. However, the *uvby* database of the LTPV project (Long-Term Photometry of Variables; Manfroid et al. 1991; Sterken et al. 1993; Manfroid et al. 1995) covers an earlier event of this kind. In order to compare the observed magnitudes and colours to model computations, these data were transformed to the *UBV* system using the relations summarized by Harmanec & Božić (2001). The results are shown in Fig. 7.

When ω CMa brightens, the $(B-V)$ colour reddens by about $+0\overset{\mathrm{m}}{.}1$, while $(U-B)$ becomes bluer by about $-0\overset{\mathrm{m}}{.}1$ (Fig. 7). This fits the behaviour described by Harmanec (1983) for a non-shell Be star. It is worth mentioning that $(U-B)$ reaches its ground state well after the V magnitude and $(B-V)$. This leads to a clear separation of the photometric ground and high state in the $(B-V)$ vs. $(U-B)$ diagram (lower panel of Fig. 7). However, this distinction is possible not only for the long-term variation but is still applicable to the short-lived brightening by less than $0\overset{\mathrm{m}}{.}1$ around JD 2 448 250. This event is confirmed at better sampling by Hipparcos, which recorded also a number of other minor events (Harmanec 1998).

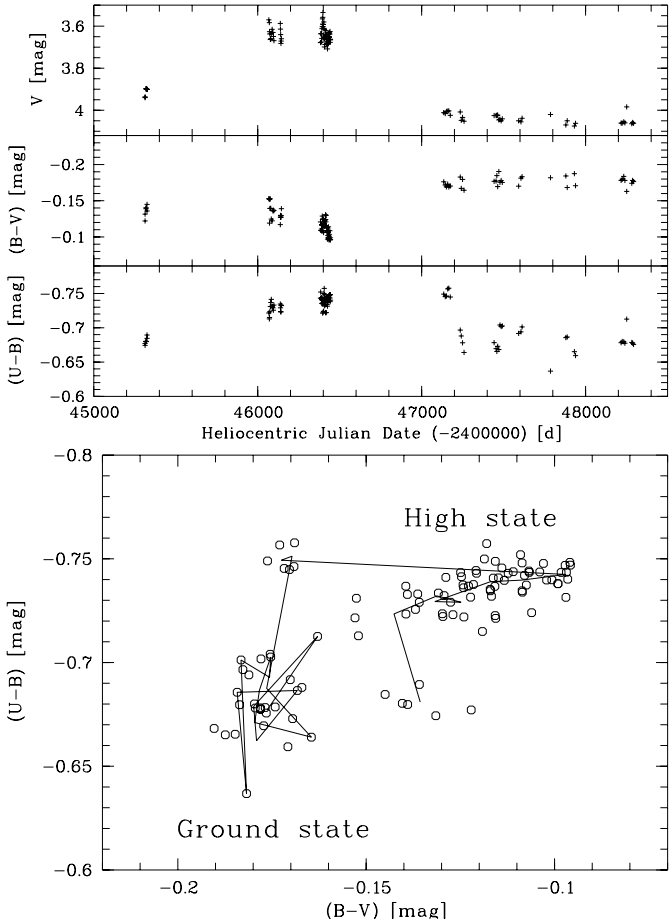

Fig. 7. LTPV observations (cf. Sect. 3.4) of ω CMa covering the rise to a photometric high state and the subsequent decline to the photometric ground state (upper panel) The corresponding path in the colour-colour diagram is shown in the lower panel. In the photometric high state, the star is red in $(B-V)$, but blue in $(U-B)$. The straight lines in the colour-colour diagram connect monthly mean values.

3.5. Balmer decrement variations

In gaseous nebulae, the Balmer decrement is a standard diagnostic for temperature and density. Using only emission components, the following quantities are defined:

$$D_{34} = f_{\rm e}({\rm H}\alpha)/f_{\rm e}({\rm H}\beta)$$
$$D_{54} = f_{\rm e}({\rm H}\gamma)/f_{\rm e}({\rm H}\beta)$$

where the line strengths $f_{\rm e}$ are in absolute flux units. In stellar spectra, line strengths are typically measured as equivalent width, i.e. normalized to the local continuum and including possible absorption components from the stellar photosphere. Before Balmer decrements can be computed for ω CMa, these effects have to be corrected for. To this end, the relations used by Dachs et al. (1990) were adopted:

$$D_{34} = W_{\rm e}({\rm H}\alpha)\, f_\star({\rm H}\alpha)/W_{\rm e}({\rm H}\beta)\, f_\star({\rm H}\beta)$$
$$D_{54} = W_{\rm e}({\rm H}\gamma)\, f_\star({\rm H}\gamma)/W_{\rm e}({\rm H}\beta)\, f_\star({\rm H}\beta)$$

where the emission equivalent width $W_{\rm e}$ is the measured total $W_{\rm tot}$ corrected for the stellar absorption $W_\star$, and $f_\star$ is the local continuum flux in absolute units.

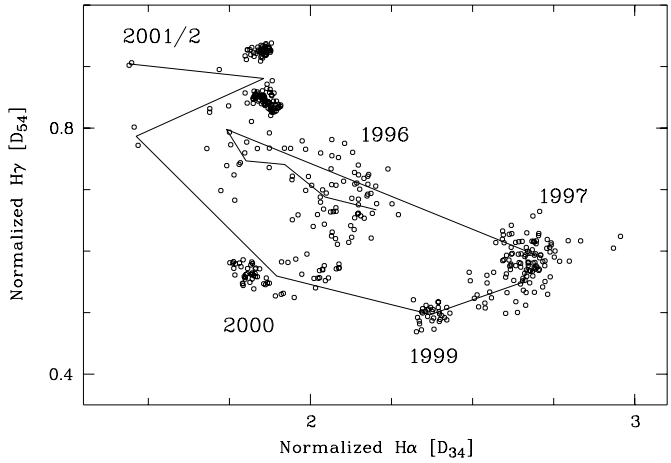

Fig. 8. Balmer decrement D_{54} vs. D_{34} diagram. The photometric ground state (1997–2000) is clearly separated from the two high states in 1996 and 2001/2002. Note that the paths between these two states seem to be direction dependent in a hysteresis-like fashion. The solid line connects monthly mean values.

In an early type B star, the flux quotients $f_\star({\rm H}\gamma)/f_\star({\rm H}\beta)$ and $f_\star({\rm H}\alpha)/f_\star({\rm H}\beta)$ are not very sensitive to the stellar parameters because the optical continuum is already well approximated by the Rayleigh-Jeans law. Therefore, model continuum fluxes for typical early type B stars computed by ATLAS 9 were used, i.e. $f_\star({\rm H}\gamma)/f_\star({\rm H}\beta) = 1.43$ and $f_\star({\rm H}\alpha)/f_\star({\rm H}\beta) = 0.35$.

The correction for the stellar contribution to the equivalent width is a more difficult matter, however. For this reason, no model calculations were relied upon but HR 4074 was adopted as a template. This star seems to be a near-twin of ω CMa, including the pulsational *lpv* (Štefl et al. 2002), except for the complete, century-long absence of line emission. Careful comparison of the spectra shows HR 4074 to be slightly cooler than ω CMa, judging from He I line wings, but still renders the star closest to ω CMa in the HEROS database. The equivalent widths adopted to correct for the photospheric components are 3.6, 4.5, and 4.7 Å for Hα, Hβ, and Hγ, respectively.

The results are presented in Fig. 8. Since the absolute values do not matter but only these quotients enter into the above equations, monochromatic continuum brightness variations do not affect the Balmer decrements. Only the colour variations (less than $0\overset{\rm m}{.}1$; cf. Sect. 3.4) introduce systematic differences of about 10% between the photometric ground and high states. This is insufficient to explain the systematic, cyclic path of ω CMa in the D_{54} vs. D_{34} diagram. Because the LTPV *UBV* photometry and the present spectroscopy do not overlap in time, no serious attempt of a correction could be made anyway.

4. Phenomena during the 2001 and other bright phases

4.1. Cyclic light and EW variations

Štefl et al. (1999) isolated the rapid photometric variations in nine seasons after smoothing the data and subtracting the

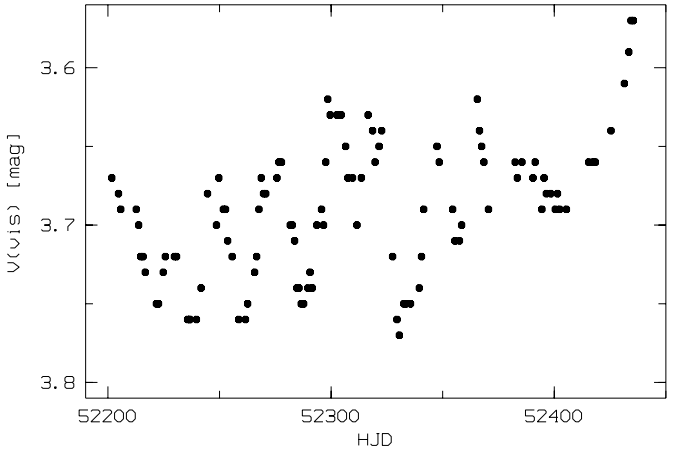

Fig. 9. Medium-term light variations during the 2001/2002 photometric maximum.

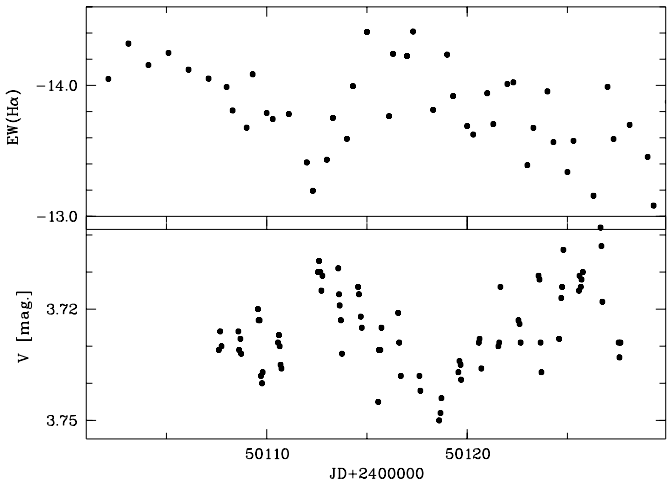

Fig. 10. Cyclic light and Hα EW variations observed during the 1996 photometric maximum. Their anti-correlation explains the Hα EW variations as an effect of the continuum variations.

medium-term variability. Although cycles of 12–15 days were apparent in some of their data sets, they could identify no common period or any correlation between cycle characteristics and emission level. They confirmed both the persistent 1.37-day and the transient 1.47-day period in the residuals. The amplitude ratio of the photospheric and transient light variations increases with brightness, i.e. mainly the transient period is present during the photometric ground state. The amplitude of the 1.37 day period increases 6–10 times, while the amplitude of the transient period only about 2 times at high brightness. Figure 9 shows variations of the visual V magnitude during the photometric maximum in the period 2001 October–2002 June. Variations with a mean cycle length of about 20 days are clearly present, although their amplitudes and the separation of maxima/minima vary by up to about 20%.

Similar variations with a quasi-period of about 25 days during the photometrically bright state have been observed by Mennickent et al. (1994) and diagnosed by them also in the earlier photometry of Balona et al. (1987).

Note that quasi-cyclic light variations were also observed already in early 2001, before the brightening, but relative maxima of about $0\overset{\mathrm{m}}{.}05$ occurred on a timescale up to twice as long.

This result prompted reanalysis of the medium-term variations in the photometric data published by Štefl et al. (2000a). Although their 3 observing runs during the 1996 photometric high state (marked N, O, P in Štefl et al. 1999, Table 1), are only 14–20 days long, the medium-term variations are well consistent with suspected cycles of 15–20 days and a peak-to-peak amplitude of $0\overset{\mathrm{m}}{.}05$–$0\overset{\mathrm{m}}{.}06$ in the Strömgren y and Geneva V passbands, respectively. The cycles were present at least between 1995 November and 1996 January. Moreover, an inspection of the other photometric data sets in Štefl et al. (1999) shows that the amplitude of the medium-term variations, too, correlates strongly with the mean brightness. Similar cycles of 12–15 days and amplitudes of $0\overset{\mathrm{m}}{.}05$–$0\overset{\mathrm{m}}{.}06$ were present also during the 1984–1986 maximum. By contrast, the range of the medium-term variations was damped to $0\overset{\mathrm{m}}{.}01$–$0\overset{\mathrm{m}}{.}02$ and their cyclic character disappeared in seasons, when the star was faint.

In summary, cyclic variations of 12–25 days duration and $0\overset{\mathrm{m}}{.}05$–$0\overset{\mathrm{m}}{.}10$ amplitude occur during the photometric high state, when also the amplitude of the periodic and transient short-term components of the light variability are increased. During the photometric ground state these medium-term variations are much reduced in amplitude.

Cyclic variations on a similar time scale of about 20 days can be observed also in the E/C ratio (see Fig. 5, upper left panel) and equivalent width of Hα monitored during the 1996 photometric maximum. The EW varies by about 7% before JD 2 450 140 and by as much as 28% later in the season. By some good fortune, the last photometric data by Štefl et al. (1999, Table 1, data set P) were obtained simultaneously with the present spectroscopy. Figure 10 shows an unambiguous correlation of the cyclic Hα and light variations. The $0\overset{\mathrm{m}}{.}05$ range in the V band corresponds to a factor 1.052 in the red continuum flux and within the errors explains well the EW variations. Since, in the same data set, variations with the same time scale could not be found in line profiles, the EW variations are entirely induced by the continuum variability.

4.2. High-redshift absorption components

During the 2001/2002 photometric high state, a distinct red absorption developed over some months at a distance of about $2\,v\sin i$ from the center of some spectral lines. It is strongest in Mg II 4481 and Si II 6347 (see Fig. 11), but still detectable also in some He I lines. It lies well outside the velocity range, where the 1.37- and 1.47-d variations have significant power. In fact, the 128 spectra of data set L, which were obtained in two consecutive nights, show no trace of such rapid variability at the position of these high-redshift features.

A specific search for a similar feature in all spectra obtained in the other seasons revealed that it was, in fact, present also during the 1996 photometric high state. It appeared and disappeared approximately at the same RV shift and on a time scale of a few days. Its position was constant, but its profile was varying on a similar time scale. Such high-redshift components were not detected in spectra taken during the photometric ground state.

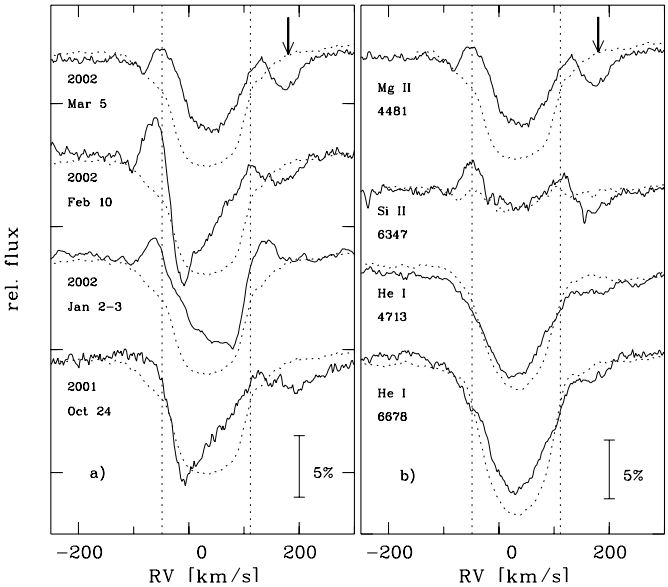

Fig. 11. Temporal development of the high-redshift absorption component in Mg II **a)** and its appearance in different spectral lines **b)**. Profiles observed during the photometric ground state (mean spectrum of the 1999 season) are overplotted as dotted lines.

5. Discussion

The above analysis has shown that the simple distinction between photometric ground and high state permits other phenomena to be associated with them:

- **Ground state:** the apparent visual magnitude is about $4\overset{m}{.}0$–$4\overset{m}{.}1$. Some flares by up to $0\overset{m}{.}2$ may occur and last up to 30 days; the repetition time could range from 200 to 300 days. All other photometric variations are difficult to detect. Hδ does not display extended wings of its emission component. FeII emission lines are basically constant, if at all present.
- **High state:** the V brightness is increased by $0\overset{m}{.}4$–$0\overset{m}{.}5$. $(B-V)$ is redder by $0\overset{m}{.}1$ and $(U-B)$ is bluer by $-0\overset{m}{.}1$. Some μ Cen-like outbursts may occur. The photometric amplitude of the 1.37-d nonradial pulsation is maximal, and photometric variations with cycle lengths of 12 to 25 days appear. The spectroscopic significance of the 1.47-d transient period becomes largest. Except for the first members of the series, Balmer emission reaches its maximum strength both in peak height and wing width. FeII lines vary significantly in strength and shape. The last 3 high states were separated by about 9 years each and lasted 1.5 to 3.5 years each.

5.1. Medium-term cycles

The cyclic light variations observed during the 1996 and 2001/2002 photometric high states have very similar quasi-periods of about 20 days. This time scale is much longer than the ones of rotation, pulsation, wind flow, etc. but much shorter than the ones of disk oscillations, precession, stellar magnetic cycles, and even of putative binary orbits (Harmanec 1998). In fact, there is no model giving only a vague hint at variations on this time scale. It is, therefore, interesting to note that this medium-term quasi-period agrees well with the beating of the photospheric 1.37-d and transient 1.47-d periods. The latter two variabilities have much increased amplitudes during the photometric bright phase while the medium-term cycles are detectable during – and probably shortly before – this phase only. This is not a proof but a welcome option to reduce the bewildering manifold of time scales at least by one.

5.2. Major and minor outbursts or only minor ones?

In the Introduction, the question was asked whether long-term variability similar to that observed in γ Cas, of which the long cycles of ω CMa could be a smaller analog, is a scaled-up version of μ Cen-like outbursts. Available observations of ω CMa do not permit a convincing answer. But one could argue that there is no indication of a continuous spectrum of events from small outbursts to long emission and light cycles as in ω CMa, not to mention γ Cas. This seems to be true also for other Be stars. The implied bimodal distribution would require (at least) two different mechanism as an explanation, which philosophically would not be attractive.

Turning to μ Cen as one of the prototypical Be stars with outbursts, it is useful to recall that in addition to the outbursts described by Rivinius et al. (1998c) μ Cen, too, undergoes long-term cycles during which the Balmer emission increases and fades. In this case, the cycle length would be of order of several decades (Rivinius 1999), and there is no associated light curve available. However, Harmanec (1983) reports it as one of the proto-type stars for the positive correlation between HI emission strength and visual brightness as described here for ω CMa. Thus, μ Cen and ω CMa might have the same kind of long-term cyclic behaviour. More importantly, the intensive long-term monitoring with very broad wavelength coverage of μ Cen did not furnish any indication of long-term variations of spectral features not formed in the disk. This, too, would suggest that the central star remains basically unchanged even during a long-term disk cycle. Accordingly, the latter would be just that, namely a cycle, which is probably driven by minor outbursts, rather than being itself an outburst on a much larger scale.

5.3. Nature of photometric long-term cycles

Extended wings in disk emission lines such as Hδ require the presence of rapidly moving/rotating matter close to the star. The close correlation of the visual brightness with the emission wings in Hδ indicates that the optical continuous radiation from the disk is produced mainly in its inner part. This is in crude quantitative agreement with the model by Poeckert & Marlborough (1978) viewed at the ω CMa inclination of about 15°: $\Delta V = -0\overset{m}{.}25$, $\Delta(B-V) = -0\overset{m}{.}08$, and $\Delta(U-B) = -0\overset{m}{.}1$ (their Fig. 30).

The Poeckert and Marlborough model was originally developed for γ Cas and has a base density (at $r = R_\star$) of $3.33 \times 10^{13}\,\mathrm{cm}^{-3}$. At such levels, the magnitude excess rises rapidly with increasing base density. Poeckert & Marlborough (1978)

do not provide an optical depth for this model. However, for a similar model of ϕ Per (Poeckert & Marlborough 1979), having a base density of $5 \times 10^{13}\,\mathrm{cm}^{-3}$, they mention an electron optical depth of the continuum of $\tau_{\mathrm{e}} = 0.37$ and a line optical depth for Hα of $\tau_{\alpha} = 30\,000$ at $r = R_{\star}$. Both numbers refer to half the geometrical thickness of the disk.

The explanation suggested by Harmanec (1998) for the long-term magnitude and colour variations invokes a "pseudo-photosphere". The primary difference to the above model by Poeckert and Marlborough is the optical thickness of the disk ($\tau > 1$ rather than $\tau < 1$). Besides, the term "photosphere" might be somewhat unfortunate since the envelope neither is spherical nor are there signs of spectral absorption lines which should be formed under LTE conditions in such a pseudo-photosphere.

Because ω CMa is viewed from a polar direction, it is, except perhaps immediately after an outburst, not obscured by the equatorial disk. Accordingly, the observed variations are due to either the disk or the star, or both, but not due to occultation-like interactions between disk and star.

Since the inner disk determines the long-term photometric behaviour, the visual brightness increases steeply after some mechanism has been started, for instance a series of outbursts, which begins to fill up the inner disk volume with mass lost from the star. Because a star of a given temperature can within a disk of a given size generate only a limited amount of continuum flux, the constancy of that temperature and size would provide a natural saturation limit to the brightenings. In fact, the amplitude of major brightenings of ω CMa is fairly constant at $0\overset{\mathrm{m}}{.}4$–$0\overset{\mathrm{m}}{.}5$ above the ground state, and some of the photometric maxima show an extended flat plateau.

With respect to Hδ and visual continuum light, the peak of the Hα emission is retarded. Presumably, this results from the combination of two effects: a) The Hα emitting region extends to larger radii, where matter arrives only later. b) This region is reached by the maximum amount of ionizing radiation only after the optical thickness of the inner disk has declined from its maximum.

5.4. Balmer decrement variations

As is well seen in Fig. 8, the D_{54} vs. D_{34} positions of the circumstellar envelope follow a circle so that the path from the photometric ground to the high state is different than the way back at the end of the cycle. This is reminiscent of the long-term colour cycle (Fig. 7). A simple scaling up and down of the disk density with phase of the long-term cycle would in both cases define only a straight line but no circle. So, obviously the disk structure is different in the transition from the ground to the high state than on the return path.

The similarity of the behaviour of the continuum (colours) and the line emission (Balmer decrements) suggests that they have similar physical and/or geometrical reasons (although it needs to be kept in mind that the zones of origin of the corresponding quantities are partly different). Such a positive correlation between continuum and line emission parameters follows also from an empirical relation found by Dachs et al. (1990) in a sample of 26 Be stars. They report (their Eq. (11)) that D_{34} is proportional to the Hα line-to-continuous emission ratio. This can be understood on the basis of both quantities being inversely proportional to the optical depth in the disk, i.e. to its electron density.

Although there is some systematic difference between the D_{34} and D_{54} values in this paper and the ones used by Dachs et al., the comparison of Fig. 8 with Figs. 1 and 2 in Dachs et al. indicates that it is relatively small: The range of Balmer decrement variations (from the ground to the high state) in ω CMa is about 2.75–1.5 and 0.5–0.9 in D_{34} and D_{54}, respectively. In the Dachs et al. sample, the corresponding ranges are about 3.0–1.1 and 0.4–1.0, of which ω CMa therefore covers about 65% each. This indicates that the physical conditions of the disk during the long-term cycle of ω CMa are in no way exceptional. Because it is probable that some of the stars of Dachs et al., too, were in various phases of long-term cycles, the similarity becomes larger still.

Theoretical models of Balmer decrements were calculated mainly for a static spherical or slab geometry, e.g. planetary nebulae. Calculations covering the parameter space appropriate for Be stars include the one by Joly (1987) for active galactic nuclei and by Williams & Shipman (1988) for rotating high-density disks around white dwarfs in cataclysmic variables. Both studies show similar qualitative dependence on the basic physical parameters of the disks, although the limiting values of corresponding Balmer decrements are different.

Balmer decrements depend only little on the temperature of the disk. However, for electron densities $10^{8}\,\mathrm{cm}^{-3} \leq n_{\mathrm{e}} \leq 10^{13}\,\mathrm{cm}^{-3}$, i.e. values typical for Be star disks, the decrements are strongly density dependent. Low D_{34} and high D_{54} values correspond to high densities. In turn, lower densities produce steep Balmer decrements, i.e. lower D_{54} and higher D_{34} values. The main trend in the transition from the photometric ground to high state, namely approximately from the lower right to the upper left corner in Fig. 8, coincides with the line representing Balmer decrement values for increasing disk density (e.g. Dachs et al. 1990, Figs. 4 and 5). From this one can crudely infer that the density in the ω CMa disk increased from about $10^{11}\,\mathrm{cm}^{-3}$ to 10^{12}–$10^{13}\,\mathrm{cm}^{-3}$. Since the hysteresis-like loops in the variability of ω CMa imply geometrical differences, affecting different quantities differently, which are not accounted for by existing models, even these differences must be looked at with some caution.

Because both the build-up and the destruction of a disk seem to progress radially outward, the mass-weighted mean radius of the disk will be smaller during the transition from photometric ground to high state than during the later return to the ground state. This is a plausible assumption for the origin of the loops in the $(U - B)$ vs. $(B - V)$ and the D_{54} vs. D_{34} diagrams.

5.5. High-redshift absorptions

The only Be star with remotely similar observations seems to be λ Eri for which Smith et al. (1991) reported an extra absorption at radial velocities of up to $+630\,\mathrm{km\,s}^{-1}$ (about $2 \times v \sin i$)

in He I 6678. However, these features only lasted for some hours, and Smith et al. interpreted them as previously ejected material falling back to the star.

The much more long-lived features in ω CMa are not explicitly predicted by any existing model. The combination of high velocity and long persistence basically excludes both the photosphere and the Keplerian disk as their place of formation. Their longevity would also be an objection to the conceivable suggestion of them being due to infall of disk matter to the star.

This would leave the wind, which is the next smaller aggregate after star and disk. Bjorkman & Cassinelli (1993) have shown that in the presence of rapid rotation wind stream lines get bent to the equator. The effect is strongest at stellar latitudes around 45°, where, in the case of a star rotating at 75% of the critical velocity, the θ component (in polar coordinates) of the streaming motion can close to the stellar surface reach 45% of the rotational velocity. Since the latter should be around 300 km s^{-1}, the right order of magnitude would be reached in absolute numbers. The small inclination, at which ω CMa is viewed, would permit a large component of this velocity to be actually picked up by the observer.

However, for the features to be in absorption, the right velocity is not sufficient. There must be a suitable continuum light source in the background. On purely geometrical grounds, one would have to assume this to be the inner disk. Section 5.3 would qualitatively support this. With the inner disk contributing significantly to the continuum flux only during the photometric high state, the absence of the high-redshift features during the photometric ground state would not imply that the wind has changed but merely that the background light source is off.

This explanation predicts that high-redshift components should be visible also in other pole-on Be stars around the times of maximum visual brightness in a long-term disk cycle. By contrast, they should even in pole-on stars not be visible during their photometric ground state and/or when their disks are very poorly developed. In fact, HR 4074, although extremely similar to ω CMa except for the century-long absence of line emission, does not show them. Also a search in spectra of other pole-on stars in the HEROS database, e.g. 31 Peg, ν Cyg or FW CMa, did not lead to the identification of similar features. However, none of these stars was observed in a phase of high brightness corresponding to the ones when ω CMa displayed high-redshift absorptions.

6. Conclusions

ω CMa undergoes correlated spectroscopic and photometric long-term variations, which in a similar form are known also for many other Be stars. Schematically, they can be abstracted as follows:

1. During a series of outbursts, more mass is temporarily pumped into the disk than is lost from it.
2. It is not known what causes these outbursts.
3. It is not known whether outbursts temporarily are more frequent or more efficient in ejecting mass from the star, or both. (In μ Cen, the long-term modulation might be explainable by assuming that two-mode beating is enough to trigger an outburst but that a beating of three or more modes controls and modulates the outburst efficiency – Rivinius 1999.)
4. It is not known how outbursts accomplish the angular momentum enrichment of the matter ending up in the disk.
5. The mass newly transferred to the disk initially accumulates mainly close to the star. It manifests itself in extended emission line wings and increased visual continuum flux while $(B-V)$ reddens and $(U-B)$ gets bluer.
6. While this continuum source is on, it could provide the background against which in pole-on stars rotationally induced wind streaming motions toward the equatorial plane can be seen at high redshift.
7. The more advanced the replenishment of the inner disk volume is, the less useful the criteria by Rivinius et al. (1998c) become for the recognition of μ Cen-like outbursts. This is so because they were established for phases of the long-term cycle of μ Cen when each outburst still had a major impact on the structure of the inner disk, i.e. when density and size were comparatively small.
8. When the inner disk volume, over which continuum radiation can be formed, is basically filled, visual maximum brightness is reached.
9. Emission lines, e.g. Hα, forming over a larger region than the visual continuum flux, attain their respective maximum later when more mass has reached those regions and they are also exposed to more ionizing flux.
10. When the inner disk is well developed, the transient 1.47-d period becomes easily detectable. The photometric amplitude of the 1.37-d *nrp* period is even more enhanced. Photometric medium-term cycles, being also confined to the photometric high state, may find their explanation in the beating of these two periods.
11. Disk destructing processes are most effective at the inner edge. When they gain higher power than the disk replenishment by outbursts, the inner disk is eroded first; extended emission line wings disappear, emission peaks shrink, and the excess continuum flux fades.
12. Eventually, when the inner disk has been swept clean, the colours and the visual flux correspond to the ones of the central star. Line emission may decrease further and at the same time be reduced to lower velocities.
13. μ Cen-like outbursts may also occur during the photometric ground state. However, their impact is small and does not last for more than 2–4 weeks.

This is the same picture as sketched in Rivinius et al. (2001) except for an extension of long-term cycles. It seems to be consistent with the observations of a fair number of other Be stars seen at small to intermediate inclination angles. For equator-on Be stars, which are more commonly known as shell stars, major brightenings become major fadings, the colour variation changes in accordance with the model of Poeckert & Marlborough (1978), and shell absorptions set in at relatively large width and low depth, thereafter narrow and deepen, and finally fade away. Finally, only stars with very small inclination would show high redshift absorption components when the inner disks provides a sufficient continuum background flux.

Acknowledgements. We thank the European Southern Observatory and University of Canterbury for generous allocations of observing time and the staff at La Silla and Mt John for their kind assistance during the observations. The allocation of guaranteed observing time of the Feros consortium, the financial support of the 1999 Heros observing run by LSW-Förderkreis and the granting of 2 nights with Feros as ESO Director General's Discretionary Time are gratefully acknowledged. John Pritchard worked very hard during the latter period in order to acquire a maximum number of spectra in service mode. Further we thank Eric Gosset, Johny Satiawan, and Chris Sterken, who obtained some supplementary Feros spectra of ω CMa during time allocated to their own projects. This work was supported by the Deutsche Forschungsgemeinschaft (Wo 296/20-1, 436 TSE 113/18) and the Academy of Sciences and Grant Agency of the Academy of Sciences of the Czech Republic (436 TSE 113/18, AA3003001, K2043105).

References

Abt, H. A., & Biggs, E. S. 1972, Bibliography of stellar radial velocities (New York: Latham Process Corp.)
Baade, D. 1979, Ph.D. Thesis, Astron. Inst. Universität Münster
Baade, D. 1982, A&A, 110, L15
Baade, D. 1984a, A&A, 135, 101
Baade, D. 1984b, A&A, 134, 105
Balona, L. A., Marang, F., Monderen, P., Reitermann, A., & Zickgraf, F.-J. 1987, A&AS, 71, 11
Bjorkman, J. E., & Cassinelli, J. P. 1993, ApJ, 409, 429
Cleminshaw, C. H. 1936, ApJ, 83, 495
Dachs, J., Kiehling, R., & Engels, D. 1988, A&A, 194, 167
Dachs, J., Rohe, D., & Loose, A. S. 1990, A&A, 238, 227
Feinstein, A. 1975, PASP, 238, 603
Harmanec, P. 1983, Hvar Obs. Bull., 7, 401
Harmanec, P. 1984, Inf. Bull. Variable Stars, 2506, 1
Harmanec, P. 1998, A&A, 234, 558
Harmanec, P., & Božić, H. 2001, A&A, 369, 1140
Harmanec, P., & Horn, J. 1998, J. Astron. Data, 4 (on CD-ROM)
Hirshfeld, A., & Sinnott, R. W. 1985, Sky catalogue 2000.0, vol. 2, Double stars, variable stars and nonstellar objects (Cambridge: Sky Publication Corp. and University Press), 15
Hubert, A. M., & Floquet, M. 1998, A&A, 335, 565
Huffer, C. M. 1939, ApJ, 89, 139
Joly, M. 1987, A&A, 184, 33
Kaufer, A. 1998, in Rev. in Mod. Astron., ed. R. E. Schielicke, 11, 177
Kaufer, A., Stahl, O., Tubbesing, S., et al. 1999, ESO Messenger, 95, 8
Kaufer, A., Wolf, B., Andersen, J., & Pasquini, L. 1997, ESO Messenger, 89, 8
Manfroid, J., Sterken, C., Bruch, A., et al. 1991, A&AS, 87, 481
Manfroid, J., Sterken, C., Cunow, B., et al. 1995, A&AS, 109, 329
Mennickent, R. E., Vogt, N., & Sterken, C. 1994, A&A, 108, 237
Okazaki, A. T. 1997, A&A, 318, 548
Otero, S., Fraser, B., & Lloyd, C. 2001, Inf. Bull. Variable Stars, 5026, 1
Perryman, M. A. C., Høg, E., Kovalevski, J., Lindgren, L., & Turon, C. 1997, The Hipparcos and Tycho Catalogues, SP-1200 (ESA)
Poeckert, R., & Marlborough, J. M. 1978, ApJS, 38, 229
Poeckert, R. 1979, ApJ, 233, 259
Rivinius, Th. 1999, Ph.D. Thesis, Ruprecht-Karls-Universität Heidelberg
Rivinius, Th., Baade, D., Štefl, S., & Maintz, M. 2001, A&A, 379, 257
Rivinius, Th., Baade, D., Štefl, S., et al. 1998a, in A Half Century of Stellar Pulsation Interpretations, ed. P. A. Bradley, & J. A. Guzik, ASP Conf. Ser., 135, 343
Rivinius, Th., Baade, D., Štefl, S., et al. 1998b, in Cyclical Variability in Stellar Winds, ed. L. Kaper, & A. A. Fullerton, ESO Conf. Ser., 207
Rivinius, Th., Baade, D., Štefl, S., et al. 1998c, A&A, 333, 125
Rivinius, Th., Štefl, S., & Baade, D. 1999, A&A, 348, 831
Slettebak, A. 1982, ApJS, 50, 55
Smith, M. A., Peters, G. J., & Grady, C. A. 1991, ApJ, 367, 302
Stagg, C. 1987, MNRAS, 227, 213
Stahl, O., Kaufer, A., & Tubbesing, S. 1999, in Optical and Infrared Spectroscopy of Circumstellar Matter, ed. E. Guenther, B. Stecklum, & K. Klose, ASP Conf. Ser., 188, 331
Stahl, O., Kaufer, A., Wolf, B., et al. 1995, Be Star Newsl., 30, 12
Sterken, C., Manfroid, J., Anton, K., et al. 1993, A&AS, 102, 79
Štefl, S., Aerts, C., & Balona, L. A. 1999, MNRAS, 305, 505
Štefl, S., Baade, D., Rivinius, Th., et al. 1998, in A Half Century of Stellar Pulsation Interpretations, ed. P. A. Bradley, & J. A. Guzik, ASP Conf. Ser., 135, 348
Štefl, S., Balona, L. A., & Aerts, C. 2000a, J. Astron. Data, 6, (on CD-ROM)
Štefl, S., Budovičová, A., Baade, D., et al. 2000b, in The Be Phenomenon in Early Type Stars, ed. M. A. Smith, H. F. Henrichs, & J. Fabregat, ASP Conf. Ser. 214, IAU Colloq., 175, 240
Štefl, S., Rivinius, Th., & Baade, D. 2002, in Radial and Nonradial Puslation as Probes of Stellar Physics, ed. C. Aerts, T. R. Bedding, & J. Christensen-Dalsgaard, ASP Conf. Ser., 259, 248
Tubbesing, S., Rivinius, Th., Wolf, B., & Kaufer, A. 2000, in The Be Phenomenon in Early Type Stars, ed. M. A. Smith, H. F. Henrichs, & J. Fabregat, ASP Conf. Ser. 214, IAU Colloq., 175, 232
van Hoof, A. 1975, Inf. Bull. Variable Stars, 992, 1
Williams, G. A., & Shipman, H. L. 1988, ApJ, 326, 738